Polyhedron 102 (2015) 176–184

Contents lists available at ScienceDirect

Polyhedron

journal homepage: www.elsevier.com/locate/poly

Synthesis, structure and SOD activity of Mn complexes with symmetric Schiff base ligands derived from pyridoxal

Sandra Signorella [a,*], Verónica Daier [a], Gabriela Ledesma [a], Claudia Palopoli [a], Davi Fernando Back [b,*], Ernesto S. Lang [b], Cristiéli Rossini Kopp [b], Patrícia Ebani [b], Mateus Brum Pereira [b], Cristiano Giacomelli [c], Paulo Cesar Piquini [d]

[a] Instituto de Química Rosario – CONICET, Facultad de Ciencias Bioquímicas y Farmacéuticas, Universidad Nacional de Rosario, Suipacha 531, S2002 LRK Rosario, Argentina
[b] Departamento de Química, Laboratório de Materiais Inorgânicos, Universidade Federal de Santa Maria, UFSM, 97115-900 Santa Maria, RS, Brazil
[c] Departamento de Química, Laboratório de Polímeros e Colóides, Universidade Federal de Santa Maria, UFSM, Santa Maria, RS, Brazil
[d] Departamento de Física, Universidade Federal de Santa Maria, UFSM, Santa Maria, RS, Brazil

ARTICLE INFO

Article history:
Received 27 July 2015
Accepted 4 September 2015
Available online 30 September 2015

Keywords:
Pyridoxal–Schiff bases
Complex Mn chelates
Superoxide activity

ABSTRACT

This study describes the synthesis, crystal structure and antioxidant activity of manganese(III) complexes with Schiff-base ligands obtained from condensation of pyridoxal with alkyl diamines: $[Mn(pyr_2en)(H_2O)_2]Cl{\cdot}4H_2O$, $[Mn(pyr_2en)(H_2O)(CH_3OH)]Cl$, $[Mn(pyr_2pn)(H_2O)_2]ClO_4$ and $[Mn_2(pyr_2bn)_3]{\cdot}4H_2O$, where H_2pyr_2en = 1,2-bis(pyridoxylidenamino)ethane, H_2pyr_2pn = 1,3-bis(pyridoxylidenamino)propane and H_2pyr_2bn = 1,4-bis(pyridoxylidenamino)butane. The four complexes catalyze the dismutation of superoxide efficiently with IC_{50} values in the range of 1.22–2.15 μM, evaluated through the nitro blue tetrazolium photoreduction inhibition superoxide dismutase assay, in aqueous solution of pH 7.8. The length of the alkyl spacer in the diamine fragment plays a key role in the antioxidant activity of these complexes, with $[Mn(pyr_2pn)(H_2O)_2]ClO_4$ showing the lowest IC_{50} value.

1. Introduction

The vast majority of living organisms need oxygen during their life cycles. During aerobic respiration, harmful reactive oxygen species (ROS) are formed [1–4]. In response, nearly all of the aerobic organisms have developed several defense mechanisms aimed at directly or indirectly minimizing the formation or spread of ROS. One of them involves antioxidant enzymes, such as superoxide dismutase (SOD) [5].

Numerous types of SOD have been found, with some of them being located in mammals. These enzymes dismutate $O_2^{\cdot-}$ radical into O_2 and H_2O_2 according to the Scheme 1, and contain metals such as Cu/Zn, Ni, Fe or Mn in their active sites [6]. The Mn-SOD enzyme is considered to be essential for mammals. Its catalytic cycle consists of a "ping-pong" type mechanism [7,8]. Its active site contains one manganese ion in a distorted trigonal bipyramidal geometry coordinated to three histidine residues, one aspartate, and one OH– ion or H_2O molecule, with a tyrosine residue in the second coordination sphere, at a distance close to 5.6 Å.

In the event of inflammatory and degenerative diseases, the production of ROS overwhelms the activity of endogenous defense systems [9]. Such an imbalance can be altered or minimized by the administration of antioxidant molecules capable of increasing cellular defense, as is the case of low molecular weight compounds able to mimic the catalytic antioxidant activity of SOD (and possibly other pharmacological requirements) [10,11].

Within this context, low molecular weight catalysts with SOD activity such as manganese complexes of the SALEN class – commonly known as EUKs – have proven to be effective in treating various types of oxidative stresses, such as ischemia reperfusion, apoptosis, and cell death of dopaminergic neurons [12,13]. Although EUKs are not the most efficient SOD-like catalysts, this class of compounds is known to have both SOD and CAT (catalase) activities in *in vitro* tests [14–16]. Such a unique characteristic renders these complexes very attractive as ROS scavengers for pharmaceutical purposes.

In this study, we report the synthesis, structural characterization and SOD activity of novel Mn complexes containing H_2pyr_2en, H_2pyr_2pn and H_2pyr_2bn ligands (Scheme 2), which are Schiff base ligands obtained by condensation of aliphatic diamines and

* Corresponding authors. Tel./fax: +54 341 4350214/+54 341 4370477 (S. Signorella). Tel.: +55 55 3220 8757; fax: +55 55 3220 8031 (D.F. Back).
E-mail addresses: signorella@iquir-conicet.gov.ar (S. Signorella), daviback@gmail.com (D.F. Back).

http://dx.doi.org/10.1016/j.poly.2015.09.007
0277-5387/

$$Mn^{3+}\text{-SOD} + O_2^{\cdot-} \longrightarrow Mn^{2+}\text{-SOD} + O_2$$

$$Mn^{2+}\text{-SOD} + O_2^{\cdot-} + 2H^+ \longrightarrow Mn^{3+}\text{-SOD} + H_2O_2$$

Scheme 1. Half reactions for the dismutation of superoxide radical mediated by Mn-SOD enzyme.

pyridoxal [17–19]. We assess the influence of the pyridoxal moiety and the role of the aliphatic spacer on the structure–activity relationship of the Mn complexes, and establish a comparison with other Mn complexes.

2. Experimental

2.1. Materials

Unless otherwise indicated, all chemicals were of the highest purity available from Sigma–Aldrich, and used without any further purification. Solvents were purified by standard methods.

2.2. Synthesis of ligands and complexes

2.2.1. Synthesis of 1,2-bis(pyridoxylidenamino)ethane hydrochloride (***H_2pyr$_2$en·2HCl***)

This ligand was prepared by modification of earlier reported synthetic procedures [20]. Pyridoxal hydrochloride (0.404 g, 2.0 mmol) dissolved in anhydrous methanol (50 mL) was reacted with 1,2-diaminoethane (0.067 mL, 1.1 mmol). The bright yellow solution was stirred during 15 min under Ar atmosphere. After evaporation of the solvent, the product was recrystallized from a mixture of methanol/water (98:2 v/v), resulting in a yellow solid. Yield = 82%. *Anal.* Calc. for $C_{18}H_{24}N_4O_4Cl_2$: C 50.12; H 5.61; N 12.98. Found: C 50.11; H 5.70; N 12.81%. Melting point: dec. 209–211 °C. IR (KBr, cm^{-1}): ν_m(O–H) 3283, ν_s(C–H)$_{ar}$2950–2900, ν_s(C=N) 1629, ν_s(C–N)$_{ar}$1261, ν_s(C–O)$_{ar}$1411, ν_s(C–O)$_{alkoh}$ 1024. ^{1}H NMR (200 MHz, DMSO-d_6): δ 8.94 (s, 2H, Py), 7.91 (s, 2H, iminic CH), 5.38 (broad s, 2H, Ar–OH,), 4.63 (s, 4H, CH_2–OH), 4.04 (s, 6H, CH_3), 3.33 (s, 2H, aliphatic OH), 2.35 (s, 4H, CH_2).

2.2.2. Synthesis of 1,3-bis(pyridoxylidenamino)propane (***H_2pyr$_2$pn***)

This ligand was synthesized through slight modification of a previously reported procedure [17,21]. Pyridoxal hydrochloride (0.404 g, 2 mmol) dissolved in dry methanol (50 mL), was reacted with potassium hydroxide (0.112 g, 2.0 mmol) and 1,3-diaminopropane (0.084 mL, 1.13 mmol). The bright yellow solution was stirred during 15 min under Ar atmosphere. After evaporation of the solvent the product was recrystallized from a mixture of methanol/ethanol (90:10 v/v), resulting a yellow–orange solid. Yield = 89%. *Anal.* Calc. for $C_{19}H_{24}N_4O_4$: C 61.29; H 6.45; N 15.05. Found: C 61.71; H 6.42; N 14.89%. Melting point: dec. 198–200 °C. IR (KBr, cm^{-1}): ν_m(O–H) 3490, ν_s(C–H)$_{ar}$2964–2940, ν_s(C=N) 1631, ν_s(C–N)$_{ar}$1310, ν_s(C–O)$_{ar}$1477, ν_s(C–O)$_{alkoh}$1016. ^{1}H NMR (200 MHz, DMSO-d_6): δ 8.91 (s, 2H, Py), 7.85 (s, 2H, iminic CH), 5.45 (broad s, 2H, Ar-OH), 4.62 (s, 2H, aliphatic OH), 3.80 (t, 4H, J = 6.6 Hz and 13.0 Hz, CH_2–OH), 2.34 (s, 6H, CH_3,), 2.16 (m, 6H, CH_2).

2.2.3. Synthesis of 1,4-bis(pyridoxylidenamino)butane (***H_2pyr$_2$bn***)

This ligand was prepared through a slight modification of an earlier reported synthetic procedure [22]. Pyridoxal hydrochloride (0.404 g, 2 mmol) dissolved in dry methanol (50 mL) was reacted with potassium hydroxide (0.112 g, 2.0 mmol) and 1,4-diaminobutane (0.10 mL, 1.13 mmol). The bright yellow solution was stirred during 15 min under Ar atmosphere. After evaporation of the solvent, the product was precipitated resulting a yellow solid. Yield = 81%. *Anal.* Calc. for $C_{20}H_{26}N_4O_4$: C 62.17; H 6.73; N 14.50. Found: C 62.01; H 6.88; N 14.49%. Melting point: dec. 188–190 °C. IR (KBr, cm^{-1}): ν_m(O–H) 3483, ν_m(C–H)$_{ar}$2912–2847, ν_s(C=N)1632, ν_s(C–N)$_{ar}$1258, ν_s(C–O)$_{ar}$1398, ν_s(C–O)$_{alkoh}$1020. ^{1}H NMR (200 MHz, DMSO-d_6): δ 8.95 (s, 1H, Py), 8.03 (s, 1H, Py), 7.83 (s, 2H, iminic CH,), 4.66 (broad s, 2H, Ar–OH,), 2.43 (s, 9H, CH_3), 2.39 (s, 3H, CH_2-OH and aliphatic OH), 1.77 (m, 4H, CH_2), 1.22 (m, 4H, CH_2). (In the Supplementary information section is the crystal structure of the ligand **H_2pyr$_2$bn**.)

2.2.4. Synthesis of [Mn(pyr$_2$en)(H_2O)$_2$]Cl·4H_2O (***1***)

H_2pyr$_2$en·2HCl (0.430 g, 1 mmol) was dissolved in methanol (8.0 mL) and mixed with manganese(II) acetate tetrahydrate

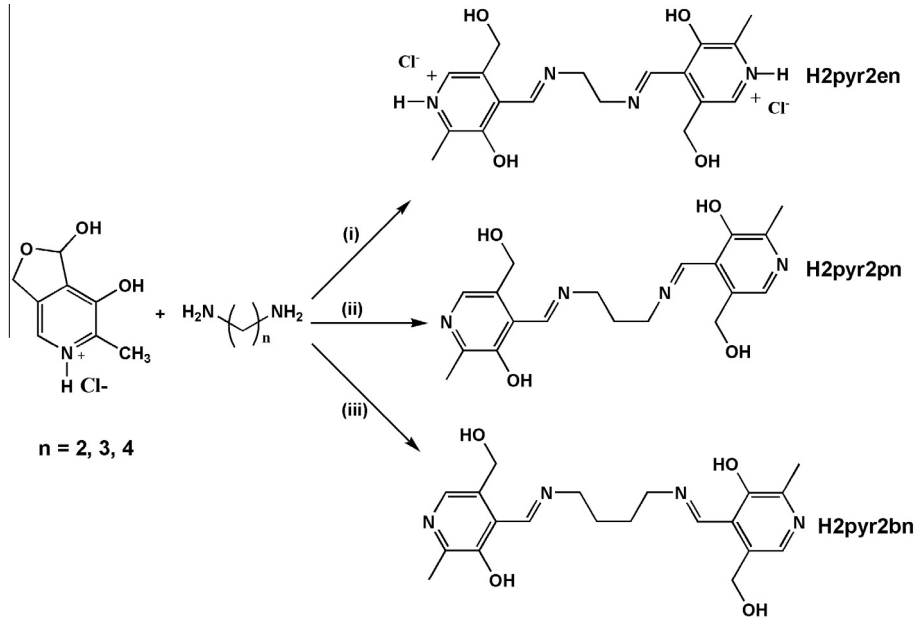

Scheme 2. Synthesis of ligands by condensation of pyridoxal with aliphatic diamines.

(98%, 0.245 g, 1 mmol). The mixture was stirred for 1.0 h at 60 °C. The precipitate was removed by filtration. Solvent evaporation yielded brown needle crystals after a few days. Yield = 48%. Melting point: 154–156 °C. *Anal.* Calc. for $C_{18}H_{32}ClMnN_4O_{10}$ (554.87 g mol^{-1}): C 38.92; H 5.76; N 10.09. Found: C 38.6; H 5.7; N 9.59%. IR (KBr, cm^{-1}): ν_m(O–H)$_{water}$3384–3200, ν_m(C–H)$_{ar}$ 2940–2924, ν_s(C=N) 1622, ν_s(C–O)$_{ar}$ 1391. UV–Vis$_{max}$ (in dimethylformamide): 420 nm (ε = 9932.6 M^{-1} cm^{-1}).

2.2.5. Synthesis of [Mn(pyr$_2$en)(H$_2$O)(CH$_3$OH)]Cl (**2**)

H$_2$pyr$_2$en·2HCl (0.430 g, 1 mmol) was dissolved in methanol (8 mL) and mixed with manganese(II) chloride tetrahydrate (99%, 0.198 g, 1 mmol). The mixture was stirred for 20 min at 60 °C. The precipitate was removed by filtration, and solvent evaporation yielded brown crystals after two days. Yield = 50%; melting point: 162–165 °C. *Anal.* Calc. for $C_{19}H_{26}ClMnN_4O_6$ (496.8 g mol^{-1}): C 45.89; H 5.23; N 11.27. Found: C 44.9; H 4.92; N 10.98%. IR (KBr, cm^{-1}): ν_s(O–H)$_{water}$ 3424–3150, ν_m (C–H)$_{ar}$,2960–2922, ν_s(=N) 1640, ν_s(C–O)$_{ar}$1492. UV–Vis$_{max}$ (in dimethylformamide): 422 nm (ε = 14464 M^{-1} cm^{-1}).

2.2.6. Synthesis of [Mn(pyr$_2$pn)(H$_2$O)$_2$]ClO$_4$ (**3**)

H$_2$pyr$_2$pn (0.372 g, 1 mmol) was dissolved in methanol (15 mL) and mixed with manganese(II) perchlorate hydrate (97%, 0.254 g, 1 mmol) (only small amounts of material should be prepared and this should be handled with care). The mixture was stirred for 10 min. at 50 °C. The solution was reserved, and solvent evaporation yielded black crystals after one day. Yield = 32%; melting point: 158–160 °C. *Anal.* Calc. For $C_{19}H_{26}ClMnN_4O_{10}$ (560.83 g mol^{-1}): C 40.65; H 4.63, N 9.98. Found: C 40.27; H 4.58, N 9.71%. IR (KBr, cm^{-1}): ν_s(O–H)$_{water}$ 3540–3474, ν_m(C–H)$_{ar}$ 2925–2850, ν_s(C=N) 1619, ν_s(C–O)$_{ar}$ 1391. UV–Vis$_{max}$: (in dimethylformamide): 367 nm (ε = 8523 M^{-1} cm^{-1}).

2.2.7. Synthesis of: [Mn$_2$(pyr$_2$bn)$_3$]·6H$_2$O (**4**)

H$_2$pyr$_2$bn (1.158 g, 3 mmol) was dissolved in methanol (25 mL) and mixed with manganese (II) acetate tetrahydrate (98%, 0.245 g, 2 mmol). The mixture was stirred during 2 h at 65 °C. The precipitate was removed by filtration, and solvent evaporation yielded black crystals after one week. Yield = 25%. Melting point: dec. 146–149 °C. *Anal.* Calc. for: $C_{60}H_{80}Mn_2N_{12}O_{16}$ (1270.28 g mol^{-1}). C 56.72; H 6.30; N 13.23. Found: C 55.81; H 6.38; N 12.99%. IR (KBr, cm^{-1}): ν_s(O–H)$_{water}$ 3490–3306, ν_m(C–H)$_{ar}$ 2921–2840, ν_s(C=N) 1613, ν_s(C–O)$_{ar}$1389. UV–Vis$_{max}$ (in dimethylformamide): 335 nm (ε = 2294 M^{-1} cm^{-1}).

2.3. X-ray crystallography

Data were collected with a Bruker APEX II CCD area-detector diffractometer and graphite-monochromatized Mo Kα radiation. The structures of the compounds **1**, **2**, **3**, **4**, and **H$_2$pyr$_2$bn** were solved by direct methods using SHELXS-97 [23]. Subsequent Fourier-difference map analyses yielded the positions of the non-hydrogen atoms. Refinements were carried out with the SHELXL-97 package [24]. All refinements were made by full-matrix least-squares on F^2 with anisotropic displacement parameters for all non-hydrogen atoms. Hydrogen atoms were included in the refinement in calculated positions except those who are commentaries by hydrogen bonds. Drawings were made with the DIAMOND for Windows [25]. Crystal data and more details of the data collections and refinements are contained in Table 1.

2.4. Physical measurements

IR spectra were measured as KBr pellets on a Shimadzu FTIR-spectrophotometer in the 4000–400 cm^{-1}region. ^{1}H NMR spectra of ligands were acquired on a Bruker DPX 200 (^{1}H at 200 MHz) in DMSO-d_6/TMS (DMSO, dimethyl sulfoxide; TMS, tetramethylsilane) solutions at 298 K. Electronic spectra were registered with Shimadzu UV 2600 spectrophotometer in the range 200–800 nm (DMF solution).

2.5. XAS experiments

X-ray absorption spectroscopy (XAS) measurements were carried out using the XAFS2 beam line at the National Synchrotron Light Laboratory (LNLS, Campinas, Brazil), which was equipped with a Si (1 1 1) single channel-cut crystal monochromator. X-ray energy was calibrated using a Mn foil (6540 eV) [26] placed after the sample. XANES spectra of Mn K-edge were recorded in air, at room temperature in transmission mode with two ion chambers as detectors located before and after the sample. Compounds as fine powder (30 mg) were mixed with boron nitride (100 mg) pressed to produce 1.0-mm thick pellets which were packed inside Kapton foils. Compounds [Mn(II)(acac)$_2$], [Mn(II)(OAc)$_2$], [Mn(III)(OAc)$_3$], Mn(IV)O$_2$ of the highest purity were used as reference in this study.

2.6. Superoxide dismutase activity

The superoxide dismutase activity (SOD activity) of complexes **1**–**4** was determined by measuring the inhibition of nitro blue tetrazolium chloride (NBT) photoreduction, according to a procedure already described [27–30]. The reaction mixture consisted of 2.4 mL of a sodium phosphate buffer solution (pH 7.8) containing 9.53×10^{-3} M methionine and 3.8×10^{-5} M NBT. Temperature was set to 25 °C. A 50 μL aliquot of a dilute solution containing complex **1**–**4** in dimethylformamide was added to the solutions, followed by addition of riboflavin (final concentration = 3.2×10^{-6} M). All experiments were done by triplicate – this included blank samples (only solvent, no added complex). The solutions were illuminated with a fluorescent lamp at constant light intensity. NBT reduction was monitored spectrophotometrically at 560 nm as a function of the illumination period (t). NBT reduction rate in the absence and in the presence of complex were determined for a range of complex concentrations. Inhibition percentage was calculated according to $\{(\Delta Abs/t)_{without\ complex} - (\Delta Abs/t)_{with\ complex}\} \times 100/(\Delta Abs/t)_{without\ complex}$. The IC$_{50}$ values represent the concentration of the SOD mimic that induces a 50% inhibition of NBT reduction. The catalytic rate constants were calculated as $k_{McCF} = k_{NBT}$ [NBT]/IC$_{50}$, where k_{NBT} (pH 7.8) = 5.94×10^4 M^{-1} s^{-1} [10].

3. Results and discussion

3.1. Structural analysis of complexes **1**–**4**

3.1.1. Complexes **1** and **2**

Reaction of H$_2$pyr$_2$en·2HCl with Mn(OAc)$_2$ or MnCl$_2$ in methanol, afforded pure complexes [Mn(pyr$_2$en)(H$_2$O)$_2$]Cl·4H$_2$O (**1**) and [Mn(pyr$_2$en)(H$_2$O)(CH$_3$OH)]Cl (**2**), respectively. Instead of the unique product obtained in neutral methanol, reaction of H$_2$pyr$_2$en·2HCl with Mn(OAc)$_2$ in basic methanol (Et$_3$N) was reported to yield a mixture of **1** and [Mn(pyr$_2$en)(EtOH)Cl] after crystallization from MeOH/EtOH [31]. X-ray diffraction analysis showed that the single-crystal structures of complexes **1** and **2** are very similar to each other (as seen in Figs. 1 and 2) and were substantially similar to the structures of EUK-8 and EUK-134 [13,32–36]. Table 1 provides additional information about the data collection and refinement of the crystal structures of complexes **1** and **2**, and the most relevant bond lengths and angles are listed in Table 2.

Table 1
Crystal data and structure refinement for the complexes **1**, **2**, **3**, **4** and the ligand **H_2pyr$_2$bn**.

Complex	**1**	**2**	**3**
Formula	C_{18} $H_{32}ClMnN_4O_{10}$	$C_{19}H_{27}ClMnN_4O_6$	$C_{19}H_{26}ClMnN_4O_{10}$
Formula weight	554.87	496.83	560.83
T (K)	290(2)	290(2)	290(2)
λ (Å)	Mo Kα; 0.71073	Mo Kα; 0.71073	Mo Kα; 0.71073
Crystal system, space group	triclinic, $P\bar{1}$	triclinic, $P\bar{1}$	monoclinic, P21/c
Unit cell dimensions			
a (Å)	8.8107(6)	8.6719(12)	12.6194(7)
b (Å)	10.8771(6)	9.0060(13)	9.3661(6)
c (Å)	13.0656(8)	14.745(2)	19.7618(14)
α (°)	100.211(4)	98.349(3)	90
β (°)	96.462(4)	94.965(3)	95.029(5)
γ (°)	91.825(4)	105.739(3)	90
V (Å^3)	1222.76(13)	1087(3)	2326.7(3)
Z, Calculated density (g cm^3)	2, 1.507	2, 1.518	4, 1.601
Absorption coefficient (mm^1)	0.708	0.774	0.745
F(000)	580	516	1160
Crystal size (mm)	0.186 × 0.139 × 0.077	0.454 × 0.091 × 0.042	0.190 × 0.104 × 0.069
Theta range for data collection θ (°)	1.60–27.27	2.39–27.53	1.62 to 27.22
Limiting indices	$-11 \leqslant h \leqslant 11$ $-13 \leqslant k \leqslant 14$ $-16 \leqslant l \leqslant 16$	$-11 \leqslant h \leqslant 11$ $-11 \leqslant k \leqslant 11$ $-19 \leqslant l \leqslant 19$	$-16 \leqslant h \leqslant 16$ $-11 \leqslant h \leqslant 12$ $-25 \leqslant h \leqslant 25$
Reflections collected/unique	28295/5587	13594/4965	18497/5062
Completeness to theta	99.9%	99.7%	99.6%
Absorption correction	numerical	numerical	numerical
Data/restraints/parameters	5587/5/307	4965/1/281	5062/1/316
Goodness-of-fit on F^2	0.959	0.963	0.995
Índice (R_{int})	0.0748	0.0879	0.1060
Final R indices [$I > 2\sigma(I)$]	$R_1 = 0.0591$, $wR_2 = 0.1496$	$R_1 = 0.0634$, $wR_2 = 0.1362$	$R_1 = 0.0624$, $wR_2 = 0.1034$
R indices (all data)	$R_1 = 0.1131$, $wR_2 = 0.1827$	$R_1 = 0.1339$, $wR_2 = 0.1694$	$R_1 = 0.1364$, $wR_2 = 0.1280$
Largest diff. peak and hole (e Å^3)	0.761–0.448	0.522–0.439	0.500–0.398

Complex	**4**	**H_2pyr$_2$bn**
Formula	$C_{30}H_{40}MnN_6O_8$	$C_{10}H_{13}N_2O_2$
Formula weight	667.62	193.22
T (K)	290(2)	290(2)
λ (Å)	Mo Kα; 0,71073	Mo Kα; 0,71073
Crystal system, space group	triclinic, $P\bar{1}$	Monoclinic, $P21/c$
Unit cell dimensions		
a (Å)	10.6944(18)	11.1948(8)
b (Å)	13.144(3)	4.9380(3)
c (Å)	13.794(3)	18.0932(12)
α (°)	62.617(9)	90
β (°)	77.712(10)	96.436(4)
γ (°)	86.725(11)	90
V (Å^3)	1680.4(5)	993.89(11)
Z, Calculated density (g cm^3)	2, 1.319	4, 1.291
Absorption coefficient (mm^1)	0.448	0.091
F(000)	694	412
Crystal size (mm)	0.099 × 0.089 × 0.036	0.276 × 0.251 × 0.108
Theta range for data collection θ (°)	2.30–26.98	2.27–27.11
Limiting indices	$-13 \leqslant h \leqslant 13$ $-16 \leqslant k \leqslant 16$ $-17 \leqslant l \leqslant 17$	$-14 \leqslant h \leqslant 14$ $-5 \leqslant k \leqslant 6$ $-23 \leqslant l \leqslant 23$
Reflections collected/unique	24578/7293	14340/2174
Completeness to theta	99.6%	99.8%
Absorption correction	numerical	numerical
Data/restraints/parameters	7293/0/408	2174/0/127
Goodness-of-fit on F^2	0.828	1.015
Índice (R_{int})	0.1068	0.0687
Final R indices [$I > 2\sigma(I)$]	$R_1 = 0.0824$, $wR_2 = 0.1440$	$R_1 = 0.0649$, $wR_2 = 0.1494$
R indices (all data)	$R_1 = 0.2584$ $wR_2 = 0.2005$	$R_1 = 0.1439$, $wR_2 = 0.1867$
Largest diff. peak and hole (e Å^3)	0.586–0.304	0.561–0.372

In complexes **1** and **2**, the ligands are polydentate with two phenolate oxygens, and two imine nitrogen atoms occupying the four equatorial coordination sites. In complex **1**, the coordination sphere is completed by two water molecules, while in complex **2** it is completed by a water molecule and a molecule of methanol. Results obtained from XANES experiments recorded in air at the Mn K-edge of complexes **1** and **2** were consistent with Mn(III) centers, thus corroborating the estimated charge for the two compounds (more details are given in the Supplementary Information section).

In the two complexes, the Mn(III) atom has a coordination number of six, adopting a slightly distorted octahedral geometry, as shown by trans angles O(3)–Mn–N(2) (174.08(12)°), O(1)–Mn–N(3) (172.50 (14)°), O(5)–Mn–O(6) (177.17(12)°) for **1** and O(3)–Mn–N(2) (172.16(15)°), O(1)–Mn–N(3) (174.81(14)°), O(5)–Mn–O(6) (171.04(13)°) for **2**. For the two complexes, Mn-N/O bond lengths and angles (Table 2) are in the range of those reported for other of Mn(III) complexes with N_2O_2-donor Schiff base ligands, with axial Mn–O distances (average Mn–O_{ax} = 2.2405

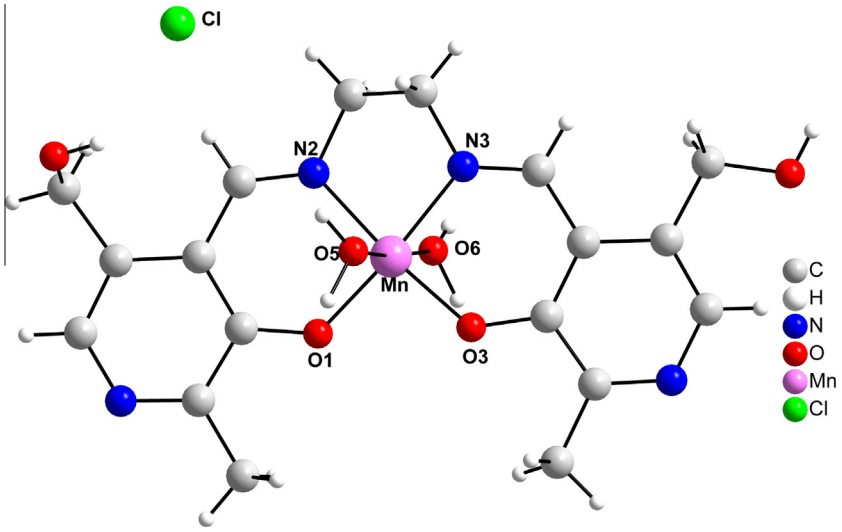

Fig. 1. Molecular structure of complex [Mn(pyr$_2$en)(H$_2$O)$_2$]Cl **(1)**. For clarity, solvates of crystallization are not shown.

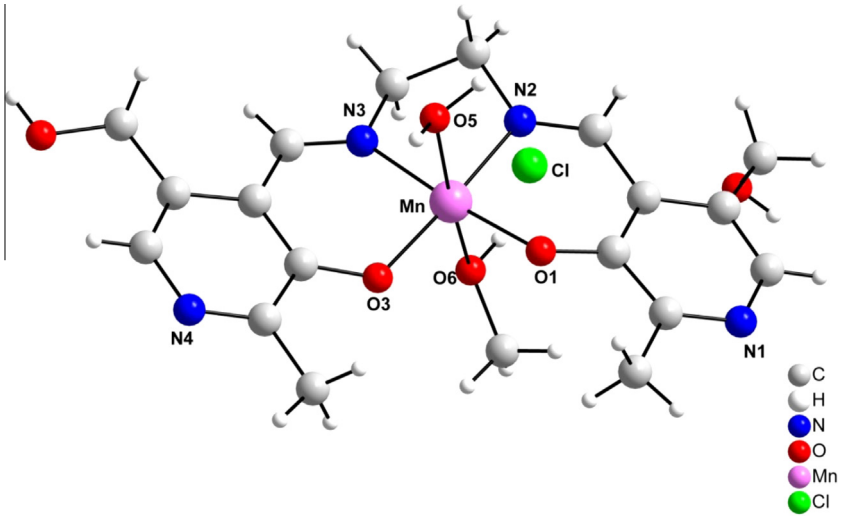

Fig. 2. Molecular structure of complex [Mn(pyr$_2$en)(H$_2$O)(CH$_3$OH)]Cl **(2)**.

Table 2
Bond distances (Å) and angles (degrees) of **1**, **2** and selected Mn-salen compounds described in the literature.

Reference	Mn–O Å (phenolic)	Mn–N Å (iminic)	Mn–L Å (axial)	O–Mn–O (°) (axial)
Complex **1** (this study)	1.862(3) 1.872(4)	1.977(4) 1.981(4)	2.218(4) 2.311(4)	175.14(13)
Complex **2** (this study)	1.863(4) 1.866(4)	1.972(4) 1.981(5)	2.214(4) 2.3207 (10)	170.66(11)
[40]	1.875(7) 1.877(7)	1.976(8) 1.977(9)	2.228(7) 2.216(7)	1 75.6(3)
[41]	1.8718(12) 1.8725(12)	1.9780(14) 1.9783(14)	2.2405 (12) 2.3257 (13)	170.10(5)
[42]	1.894(1) 1.886(1)	1.984(2) 1.974(2)	2.347(2) 2.125(2)	173.90(5)
[43]	1.8818(6) 1.8964(6)	1.9981(7) 1.9739(7)	2.1947(7) 2.2324(7)	177.95(2)

(6) Å) considerably longer than the equatorial ones, owing to Jahn–Teller distortion of the high-spin Mn(III) system [37–43].

Compound **2**, which contains a chloride anion but no hydration water molecules, displays a two-dimensional supramolecular arrangement promoted by intermolecular hydrogen bonds of trifurcated donor type, with three receivers [44]. The distances between the atoms involved in the trifurcated interactions (along the crystallographic direction [010]) [45–47] in the dimers (Fig. 3) of complex **2** are 2.845(5), 2.837(5) and 2.275(3) Å for H8#···Cl, H10B···Cl, and H6D···Cl, respectively.

3.1.2. Complex *3*

In the case of complex [Mn(pyr$_2$pn)(H$_2$O)$_2$]ClO$_4$ (**3**), shown in Fig. 4, featuring a propylene spacer between pyridoxal moieties, the ligand is also polydentate, with the two phenolate oxygens and two iminic nitrogens in the equatorial positions. The coordination sphere of complex **3** is completed by two molecules of water in the two trans-axial sites. The asymmetric unit also contains a perchlorate as counter ion. The trans angles at the metal center are O(3)–Mn–N(2) (177.72°), N(3)–Mn–O(1) (177.25°) and O(6)–Mn–O(5) (176.61°), implying a slightly distorted octahedron around the Mn ion.

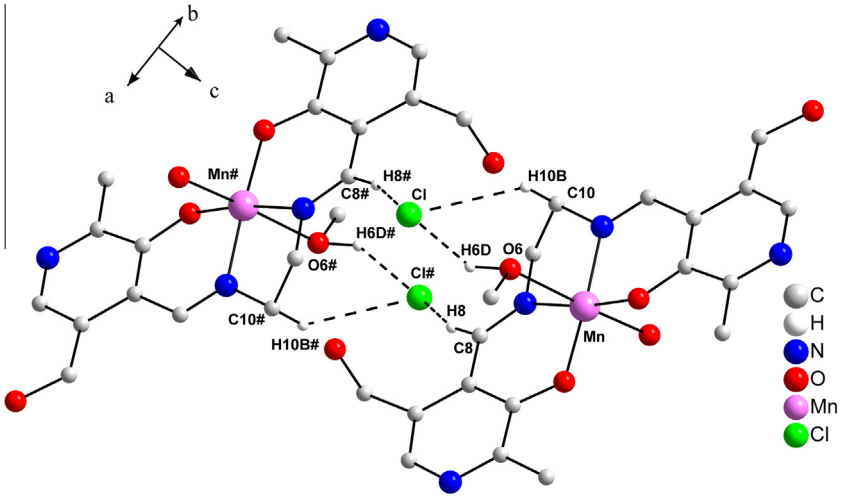

Fig. 3. Trifurcated hydrogen interactions in complex **2**. Symmetry operations used to generate equivalent atoms: (#) 1 – *x*, 1 – *y*, 1 – *z*.

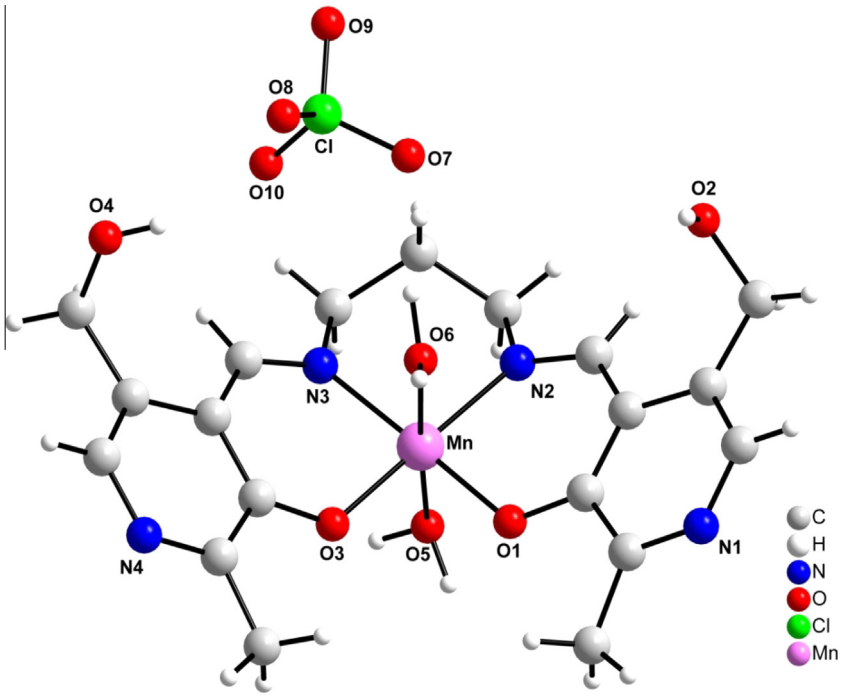

Fig. 4. Molecular structure of complex $[Mn(pyr_2pn)(H_2O)_2]ClO_4$ (**3**).

The bond distance values from the metal center to the imine nitrogen and the oxygen atoms of phenolate are in accordance with those of Mn-salpn complexes [48–50]. The most relevant values for the bond lengths and angles are listed in Table 3. For this complex, the oxidation state of the metal determined by XANES measurements is consistent with Mn(III) centers, similarly to complexes **1** and **2** shown above (see Supplementary Information section).

Pyr_2pn^{2-} possesses one additional methylene spacer in the diamine fragment which confers flexibility to the ligand backbone, compared to pyr_2en^{2-} in **1** and **2**. Thus, instead of the relatively planar conformation of the pyr_2en^{2-} ligand in **1** and **2**, pyr_2pn^{2-} adopts a dome-shaped conformation in **3** with Mn-ligand bond lengths slightly longer than in **1** and **2**. The same difference was observed between salpn-Mn [45–47] and salen-Mn [40–43] complexes.

The oxygen atoms of the perchlorate ion promotes an increase in inter- and intramolecular hydrogen bonding strength between H4···O10, O7···H06a, H05a#···O8, and H8#2···O9#2 (Fig. 5), with distances between the atoms of 2.090(9), 2.013(9), 2.112(9), and 2.484(9) Å respectively.

Table 3
Selected bond distances (Å) and angles (degrees) for complexes **3** and **4**.

3		**4**	
Bond distances (Å)			
Mn-N(2)	2.019(3)	Mn–N(2)	2.230(6)
Mn-N(3)	2.035(3)	Mn–N(3)	2.035(6)
Mn–O(1)	1.882(3)	Mn–N(6)	2.326 (5)
Mn–O(3)	1.879(3)	Mn–O(1)	1.887 (4)
Mn–O(5)	2.191(3)	Mn–O(3)	1.927 (4)
Mn–O(6)	2.244(3)	Mn–O(5)	1.917 (4)
Bond angles (°)			
O(3)–Mn–N(2)	177.76 (13)	O(5)–Mn–O(3)	176.1(2)
O(1)–Mn–N(3)	177.19 (13)	N(6)–Mn–N(2)	168.3 (2)
O(5)–Mn–O(6)	176.28 (11)	N(3)–Mn–O(1)	176.6 (2)

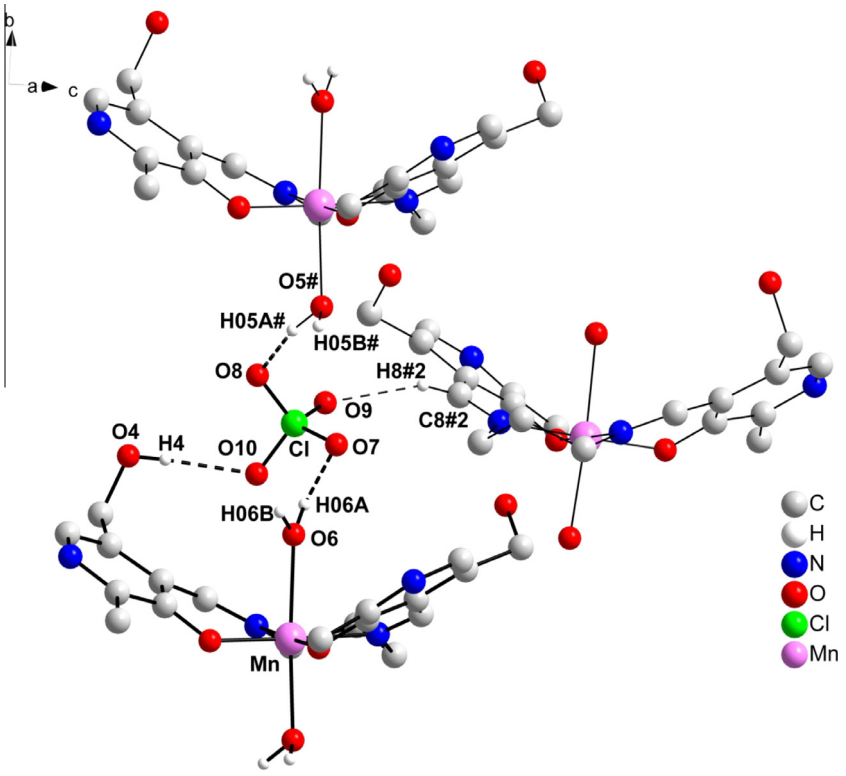

Fig. 5. DIAMOND plot of complex **3** with the atom numbering. Symmetry code for the generated atoms: # x, 1 + y, z; # 2 − x, 0.5 + y, 1.5 − z. For the sake of clarity, hydrogen atoms not involved in secondary bonds (dashed lines) are omitted.

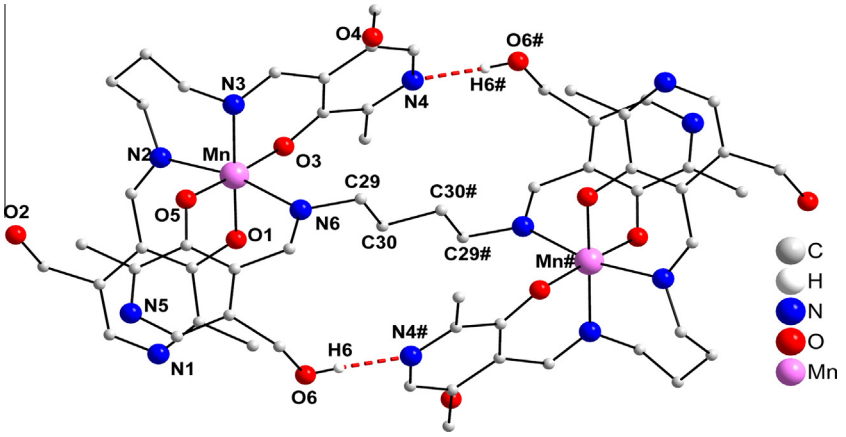

Fig. 6. DIAMOND plot of complex **4** with the atom numbering. Symmetry code for the generated atoms: # −x, 1 − y, −z. For clarity the hydrogen atoms not involved in secondary bonds (dashed lines) are omitted.

Table 4
Selected H-bond distances and intramolecular bond angles for compound **4**.

(D–H···A)	D–H (Å)	H···A (Å)	D···A (Å)	D–H···A (°)
O6–H6···N4#	0.820(7)	2.046(8)	2.790(13)	150.62(35)

3.1.3. Complex *4*

The structure of complex **4** is shown in Fig. 6, and is well different from those discussed above. It consists in a neutral molecule composed of three pyr_2bn^{2-} ligands and two Mn ions. The pyr_2bn^{2-} ligand binds the metal through two phenolate oxygen and two imine nitrogen atoms. The coordination sphere of Mn in

Table 5
IC_{50} values and rate constants for complexes **1**–**4**.

Complex/reference	IC_{50} (μM)	k_{McCF} (M^{-1} s^{-1}) × 10^6
1	2.11	1.06
2	2.15	1.04
3	1.22	1.84
4	1.78*	1.26*
[28]	1.14	2.4
[16]	1.43	1.91
[59]	1.33	11.05
[60]	2.93	4.6
[61]	3.73	not reported
[64]	1.26	1.7

* Per Mn site.

complex **4** is completed by one phenolate oxygen atom and one imine nitrogen atom from a second molecule of the ligand that is shared by the two metal centers. The Mn ion shows a distorted octahedral coordination geometry, as evidenced by the angles O(5)–Mn–O(3) (176.28°), N(6)–Mn–N(2) (167.32°), and N(3)–Mn–O(1) (176.84°). Mn–N/O equatorial distances (Mn–O/N_{eq} 1.928 Å) are shorter than axial Mn–N bond lengths (Mn–N_{ax} = 2.217 and 2.323 Å), in agreement with values reported for other Mn(III) complexes [48,51–53]. Table 1 summarizes information on the data collection and refinement of the crystal structure of complex **4**. Additional bond lengths and angles are listed in Table 3. In this case, the butylene spacer between the two imino nitrogen atoms imparts this ligand with enough flexibility to assume a *β-cis* folded configuration [16]. This arrangement allows a second ligand molecule to occupy two *cis* sites in the coordination sphere of the Mn ion.

The strength of hydrogen interactions in complex **4** is moderate as judged from bond distances shown in Table 4. Bond distances and angles (close to 150°) are in agreement with the models proposed by Steiner and Jeffrey [42,54].

3.2. SOD activity

SOD activity of complexes **1**–**4** was determined at pH 7.8 by the NBT photoreduction method. The four complexes inhibited the reduction of NBT with increasing inhibition as the concentration of complexes increased. IC_{50} values summarized in Table 5 reveal that their antioxidant activity is in the range of other MnSOD mimics with open chain ligands, including salen and salpn-type Mn complexes [10,28,13,32–36,40,55–60] and is clearly higher than that of well-known stoichiometric antioxidants such as mannitol and vitamin C [62,63].

Complexes **1** and **2** showed essentially the same antioxidant activity, as expected from the fact that their molecular structures are similar. In both cases, the complexes have short equatorial Mn–N and Mn–O bonds and longer axial Mn–O bonds, occupied by two water molecules in **1** or by water and methanol in **2**, affording labile substitution sites to interact with the substrate. Therefore, complexes **1** and **2** are analogous in solution, as the IC_{50} data clearly reflect.

Replacing the ethylene spacer between pyridoxal units with a propylene chain resulted in complex **3** with 25° deviation from planarity of the central polyhedron and the pyridoxal molecules. Whilst still maintaining two water molecules coordinated to the metallic center at the axial positions, complex **3** revealed a noticeably lower IC_{50} value of 1.22 μM as compared to **1** and **2** ($IC_{50} \sim 2.1$ μM). The higher reactivity of **3** can result from its dome-shaped octahedral geometry**,** in which one of the axial ligands is very weakly coordinated, thus favoring ligand exchange and interaction with the substrate.

In complex **4**, the six coordination sites of the metal are occupied by donor sites of the ligand. Thus, initial binding to the substrate must occur through ligand shift, the most probable being the shift of the weakly bound N6-imino group. This ligand replacement should slow down the SOD rate (compared to complexes where a solvent molecule is replaced). However, the high flexibility of the butylene moiety facilitates the ligand shift affording an IC_{50} lower than for complexes **1**–**2** (with a more rigid C2 unit) and similar to that observed for other Mn complexes of hexadentate N_3O_3 ligands [64].

Values of the catalytic rate constants for superoxide disproportionation shown in Table 5 clearly indicates that these complexes can be used as superoxide scavengers. Comparison of k_{McCF} of complexes **1**–**4** reveal that the geometry around Mn contributes to modulate SOD activity, with **3** being the best suited to react with superoxide.

4. Conclusions

The condensation of 1,n-diamines with pyridoxal afforded Schiff bases, which were very efficient for coordination to manganese(III).

The results indicated that, with the increasing length of the organic spacers, the coordination geometry of complex **4** was significantly modified, forming a neutral complex with the six coordination positions of Mn occupied by ligand donor sites; whereas the other complexes (**1**, **2**, and **3**) were positively charged with coordinated solvent molecules.

The four complexes are effective SOD mimics with catalytic acitivity in the range of other Mn complexes with open chain ligands. In Mn-py_2pn (**3**) the bending of the tetradentate ligand leads to a weakly coordinated exchangeable axial solvent molecule which facilitates substrate binding. Thus, this complex is the best suited to react with superoxide and shows the lowest IC_{50} value among the compounds evaluated in this study. These results emphasize the role played by the geometry around the metal ion in the reaction with superoxide.

Acknowledgments

Brazilian Research Councils: CNPq – Edital No. 14/2011 and Edital 11/2014 (Proc. 444780/2014-9); FAPERGS – Fundação de Amparo à Pesquisa do Estado do Rio Grande do Sul – Edital No. 002/2011 – PqG and MINCyT and CAPES for a Bilateral Cooperation Program (Project No. BR/09/19).

Appendix A. Supplementary data

CCDC-1415373, 1415374, 1415375, 1415376 and 1415377 contain the supplementary crystallographic data for the complexes **1, 2, 3, 4** and the ligand **H_2pyr$_2$bn** respectively. These data can be obtained free of charge via http://www.ccdc.cam.ac.uk/conts/retrieving.html, or from the Cambridge Crystallographic Data Centre, 12 Union Road, Cambridge CB2 1EZ, UK; fax: (+44) 1223–336–033; or e–mail: deposit@ccdc.cam.ac.uk. Supplementary data associated with this article can be found, in the online version, at http://dx.doi.org/10.1016/j.poly.2015.09.007.

References

[1] D. Harman, Ann. N.Y. Acad. Sci. 786 (1996) 321.
[2] A. Puglisi, G. Tabbì, G. Vecchio, J. Inorg. Biochem. 98 (2004) 969.
[3] L.M. Walker, J.L. York, S.Z. Imam, S.F. Ali, K.L. Muldrew, P.R. Mayeux, Toxicol. Sci. 63 (2001) 143.
[4] G.I. Giles, K.M. Tasker, C. Collins, N.M. Giles, E. O'Rourke, C. Jacob, Biochem. J. 364 (2002) 579.
[5] G. Lupidi, F. Marchetti, N. Masciocchi, D.L. Reger, S. Tabassum, P. Astolfi, E. Damiani, C. Pettinari, J. Inorg. Biochem. 104 (2010) 820.
[6] D.M. Moreno, M.A. Martí, P.B. De Biase, D.A. Estrin, V. Demicheli, R. Radi, L. Boechi, Arch. Biochem. Biophys. 507 (2011) 304.
[7] C. Bull, E.C. Niederboffer, T. Yoshida, J.A. Fee, J. Am. Chem. Soc. 113 (1991) 4069.
[8] C.K. Vance, A. Miller, Biochemistry 37 (1998) 5518.
[9] J.M. Matés, Toxicology 153 (2000) 83.
[10] S. Durot, C. Policar, F. Cisnetti, F. Lambert, J.F. Renault, G. Pelosi, G. Blain, H.K. Youssoufi, J.P. Mahy, Eur. J. Inorg. Chem. 17 (2005) 3513.
[11] G.I. Grasso, G. Arena, F. Bellia, E. Rizzarelli, G. Vecchio, J. Inorg. Biochem. 131 (2014) 56.
[12] F. Fucassi, J.E. Lowe, K.D. Pavey, S. Shah, R.G.A. Faragher, M.H.L. Green, F. Paul, D.O'. Hare, P.J. Cragg, J. Inorg. Biochem. 101 (2007) 225.
[13] W. Munroe, C. Kingsley, A. Durazo, E.B. Gralla, J.A. Imlay, C. Srinivasan, J.S. Valentine, J. Inorg. Biochem. 101 (2007) 1875.
[14] G.M.P. Giblin, P.C. Box, I.B. Campbell, A.P. Hancock, S. Roomans, G.I. Mills, C. Molloy, G.E. Tranter, A.L. Walker, S.R. Doctrow, K. Huffmand, B. Malfroyd, Bioorg. Med. Chem. Lett. 11 (2001) 1367.
[15] Q. Li, Q. Luo, Y. Li, Z. Pan, M. Shen, Eur. J. Inorg. Chem. 22 (2004) 4447.
[16] V. Daier, D. Moreno, C. Duhayon, J. Tuchegues, S. Signorella, Eur. J. Inorg. Chem. 6 (2010) 965.

[17] D.F. Back, G.M. Oliveira, J.P. Vargas, E.S. Lang, G. Tabarelli, J. Inorg. Biochem. 102 (2008) 666.
[18] M.R. Maurya, P. Saini, A. Kumar, J.C. Pessoa, Eur. J. Inorg. Chem. 31 (2011) 4846.
[19] J.S. Casas, A. Castiñeiras, F. Condori, M.D. Couce, U. Russo, A. Sánchez, R. Seoane, J. Sordo, J.M. Varela, Polyhedron 22 (2003) 53.
[20] I. Correia, J.C. Pessoa, M.T. Duarte, R.T. Henriques, M.F.M. Piedade, L.F. Veiros, T. Jakusch, T. Kiss, Á. Dönyei, M.M.C.A. Castro, C. F.G.C. Geraldes, F. Avecilla, Chem. Eur. J. 2004, 10, 2301–2317. S. Naskar, S. Naskar, R.J. Butcher, S.K. Chattopadhyay, Inorg. Chim. Acta 363, 2010, 404–411.
[21] H. Eshtiagh-Hosseini, M.R. Housaindokht, S.A. Beyramabadi, S. Beheshti, A.A. Esmaeili, M.J. Khoshkholgh, A. Morsali, Spectrochim. Acta Part A Mol. Biomol. Spectrosc. 71 (2008) 1341.
[22] H. Eshtiagh-Hosseini, M.R. Housaindokht, S.A. Beyramabadi, S.H.M. Tabatabaei, A.A. Esmaeili, M.J. Khoshkholgh, Spectrochim. Acta Part A Mol. Biomol. Spectrosc. 78 (2011) 1046.
[23] G.M. Sheldrick, SHELXS-97: Program for Crystal Structure Solution, University of Göttingen, Germany, 1997.
[24] G.M. Sheldrick, SHELXL-97: Program for Crystal Structure Refinement, UniversityofGöttingen, Germany, 1997.
[25] K. Brandenburg, DIAMOND 3.1a. 1997–2005, Version 1.1a. Crystal Impact GbR, Bonn, Germany.
[26] H. Visser, E. Anxolabéhère-Mallart, U. Bergmann, P. Glatzel, J.H. Robblee, S.P. Cramer, J. Girerd, K. Sauer, M.P. Klein, V.K. Yachandra, J. Am. Chem. Soc. 123 (2001) 7031.
[27] C. Beauchamps, I. Fridovich, Anal. Biochem. 44 (1971) 276.
[28] D. Moreno, V. Daier, C. Palopoli, J.-P. Tuchagues, S. Signorella, J. Inorg. Biochem. 104 (2010) 496.
[29] O. Iranzo, Bioorg. Chem. 39 (2011) 73.
[30] B. Verdejo, S. Blasco, E. García-España, F. Lloret, P. Gaviña, C. Soriano, S. Tatay, H.R. Jiménez, A. Doménech, J. Latorre, Dalton Trans. 41 (2007) 4726.
[31] S. Naskar, S. Naskar, R.J. Butcher, M. Corbella, A. Espinosa Ferao, S.K. Chattopadhyay, Eur. J. Inorg. Chem. (2013) 3249.
[32] J.J. Collins, K. Evason, K. Kornfeld, Exp. Geront. 41 (2006) 1032.
[33] K. Pong, S.R. Doctrow, K. Huffman, C.A. Adinolfi, M. Baudry, Exp. Neurol. 171 (2001) 84.
[34] M. Keaney, F. Matthijssens, M. Sharpe, J. Vanfleteren, D. Gems, Free Radic. Biol. Med. 37 (2004) 239.
[35] M. Baudry, S. Etienne, A. Bruce, M. Palucki, E. Jacobsen, B. Malfroy, Biochem. Biophys. Res. Commun. 192 (1993) 964.
[36] A. Bayne, R.S. Sohal, Free Radic. Biol. Med. 32 (2002) 1229.
[37] K. Mitra, S. Biswas, C.R. Lucas, B. Adhikary, Inorg. Chim. Acta 359 (2006) 1997.
[38] C.J. Sanders, P.N. O'Shaughnessy, P. Scott, Polyhedron 22 (2003) 1617.
[39] M. Maiti, D. Sadhukhan, S. Thakurta, E. Zangrando, G. Pilet, A. Bauzá, A. Frontera, B. Dede, S. Mitra, Polyhedron 75 (2014) 40.
[40] M.R. Bermejo, A. Castiñeiras, J.C. Garcia-Monteagudo, M. Rey, A. Sousa, M. Watkinson, C.A. McAuliffe, R.G. Pritchard, R.L. Beddoes, J. Chem. Soc., Dalton Trans. 14 (1996) 2935.
[41] M.Á. Vázquez-Fernández, M.I. Fernández-García, A.M. González-Noya, M. Maneiro, M.R. Bermejo, M.J. Rodríguez-Doutón, Polyhedron 31 (2012) 379.
[42] M. Sutradhar, L.M. Carrella, E. Rentschler, Polyhedron 38 (2012) 297.
[43] M. Allard, R. Ricoux, R. Guillot, J. Mahy, Inorg. Chim. Acta 382 (2012) 59.
[44] D.F. Back, M. Hörner, F. Broch, G.M. Oliveira, Polyhedron 31 (2012) 558.
[45] D. Ghoshal, A.K. Ghosh, J. Ribas, G. Mostafa, N.R. Chaudhuri, Cryst. Eng. Comm. 7 (2005) 616.
[46] T. Steiner, Angew. Chem., Int. Ed. 41 (2002) 48.
[47] S.K. Panigrahi, G.R. Desiraju, Proteins Struct. Funct. Bioinf. 67 (2007) 128–141.
[48] K.R. Reddy, M.V. Rajasekharan, J.-P. Tuchagues, Inorg. Chem. 37 (1998) 5978.
[49] S. Sailaja, K. Rajender Reddy, M.V. Rajasekharan, C. Hureau, E. Rivière, J. Cano, J.-J. Girerd, Inorg. Chem. 42 (2003) 180.
[50] I. Hwang, K. Ha, Acta Cryst. E63 (2007) m2337.
[51] J. Costes, F. Dahan, B. Donnadieu, M.R. Douton, M.F. Garcia, A. Bousseksou, J. Tuchagues, Inorg. Chem. 43 (2004) 2736.
[52] M. Okuhata, T. Mochida, Polyhedron 43 (2012) 153.
[53] R. Uhrecký, Z. Padělková, J. Moncol, M. Koman, L. Dlháň, J. Titiš, R. Bocă, Polyhedron 56 (2013) 9.
[54] G.A. Jeffrey, An Introduction to Hydrogen Bonding, University Press, Oxford, 1997.
[55] D. Salvemini, D.P. Riley, P.J. Lennon, Z. Wang, M.G. Currie, H. Macarthur, T.P. Misko, Br. J. Pharmacol. 127 (1999) 685.
[56] F.C. Friedel, D. Lieb, I. Ivanović-Burmazović, J. Inorg. Biochem. 109 (2012) 26.
[57] S.R. Doctrow, K. Huffman, C. Bucay Marcus, G. Tocco, E. Malfroy, C.A. Adinolfi, H. Kruk, K. Baker, N. Lazarowych, J. Mascarenhas, B. Malfroy, J. Med. Chem. 45 (2002) 4549.
[58] Y. Noritake, N. Umezawa, N. Kato, T. Higuchi, Inorg. Chem. 52 (2013) 3653.
[59] J. Bian, Y. Wang Wei, J. Tang, Fu-P. Huang, D. Yao, Q. Yu, H. Liang, Polyhedron 90 (2015) 147–153.
[60] J. Lin, C. Tu, H. Lin, P. Jiang, J. Ding, Z. Guo, Inorg. Chem. Commun. 6 (2003) 262.
[61] K. Ghosh, N. Tyagi, P. Kumar, Inorg. Chem. Commun. 13 (2010) 380.
[62] N. Yilmaz, H. Dulger, N. Kiymaz, C. Yilmaz, B.O. Gudu, I. Demir, Brain Res. 1164 (2007) 132.
[63] D.S. Raja, G. Paramaguru, N.S.P. Bhuvanesh, J.H. Reibenspies, R. Renganathan, K. Natarajan, Dalton Trans. 40 (2011) 4548.
[64] G.N. Ledesma, H. Eury, E. Anxolabéhère-Mallart, C. Hureau, S.R. Signorella, J. Inorg. Biochem. 146 (2015) 69.